Accepted manuscript doi:
10.1680/jgele.21.00063

Submitted: 30 May 2021

Published online in 'accepted manuscript' format: 15 October 2021

Manuscript title: Relationship between pore size distribution and compressibility of a lateritic soil

Authors: Vinícius de Oliveira Kühn[1], Bruna de Carvalho Faria Lima Lopes[2], Camilla Rodrigues Borges[3], Narayana Saniele Massocco[4] and Manoel Porfírio Cordão Neto[4]

Affiliations: [1]Centre for Exact Sciences and Technology, Federal University of Western Bahia, Barreiras, Brazil; [2]Department of Civil and Environmental Engineering, University of Strathclyde, Glasgow, UK; [3]Federal Institute of Goiás, Campus Luziânia, Goiânia, Brazil and [4]Civil and Environmental Engineering Department, University of Brasilia, Faculty of Technology, Brasília, Brazil

Corresponding author: Vinícius de Oliveira Kühn, Centre for Exact Sciences and Technology, Federal University of Western Bahia, Barreiras, Brazil.

E-mail: vinicius.kuhn@ufob.edu.br

Downloaded by [University of Strathclyde] on [22/10/21]. Copyright © ICE Publishing, all rights reserved.

Accepted manuscript doi:
10.1680/jgele.21.00063

Abstract

The aim of this paper is the evaluation of the relationship between pore size distribution and compressibility of a lateritic soil. Soil fabric was analysed under different conditions of preparation: compacted, reconstituted, and intact, by means of Mercury Intrusion Porosimetry tests upon loading to different stress levels. Results show that all samples present bimodal pore distribution. However, the conditions of preparation and loading affected macropores more intensely, with subtle effects on micropores. This behaviour was attributed to the presence of aggregations with cementation. The compression curve of macro and micropores were determined and it was observed that the compression curve of macropores is very similar to the compression curve of the samples. In addition, it was observed that the fabric parameter regarding the uniformity of macro and micropores changed during loading. The new fabric parameter proposed captures the change in pore uniformity with loading. This parameter appears to be related to the soil compressibility, indicating that the most compressible samples also show greater changes in the uniformity of macropores.

Keywords: Compressibility; Fabric of soils; Lateritic soils

Downloaded by [University of Strathclyde] on [22/10/21]. Copyright © ICE Publishing, all rights reserved.

Accepted manuscript doi:
10.1680/jgele.21.00063

1. Introduction

Geotechnical studies carried out over the years have shown that there is a relationship between the mechanical behaviour of soils and their microstructure, mainly in terms of compressibility (Alonso, Pinyol & Gens, 2013; Lambe & Whitman, 1969; Delage *et al.*, 2006; Koliji, Vulliet & Laloui, 2010; Ng, Mu & Zhou, 2017; Yu, Chow & Wang, 2016; Ng, Akinniyi & Zhou, 2020; Kochmanová & Tanaka, 2011; Sivakumar & Wheeler, 2000; Ng *et al.*, 2020; Wang *et al.*, 2020). The fabric effect on compressibility can be observed by carrying out tests on samples prepared under different initial conditions, such as: intact, compacted and reconstituted (Burland, 1990; Leroueil & Vaughan, 1990), where changes in behaviour are observed in terms of compression indexes and preconsolidation stresses. Microstructural evaluation based on Mercury Intrusion Porosimetry (MIP) and Scanning Electron Microscopy (SEM) tests has been used to measure soil fabric quantitatively and qualitatively. Soil fabric can assume pore size distributions that vary from mono-modal to multi-modal (more than two dominant pore sizes), however mono-modal and bimodal (two dominant pore sizes) distributions are the most widely reported (Kühn *et al.*, 2021; Romero, 2013; Pedrotti & Tarantino, 2014; Miguel & Bonder, 2012; Delage *et al.*, 1996). Highly weathered lateritic tropical soils present bimodal pore size distributions for both intact and compacted samples (Santos & Esquivel, 2018; Otálvaro, Cordão-Neto & Caicedo, 2015; Cordão Neto *et al.*, 2018). These soils are distinguished by their mineralogical composition, with marked presence of iron and aluminium oxides and hydroxides (Otálvaro *et al.*, 2016; Mitchell & Soga, 2005; Miguel & Bonder, 2012) which contributes to the formation of aggregations in their structure (Camapum de Carvalho *et al.*, 2006).

Despite many studies analysing jointly the distribution of pores and the mechanical behaviour of soils, there is no constitutive relationship between mechanical and porosimetry parameters. In this sense, the aim of this paper is the evaluation of the relationship between pore size distribution and compressibility of a lateritic soil. For this, a series of MIP tests were performed on samples prepared under different conditions, namely: Intact, Compacted, and Reconstituted, and loaded unidimensionally to different stress levels. Using a fitting equation, the void ratio and the compression index of macro- and micropores were separated, and a new fabric parameter was proposed. In this way, this paper presents a new approach to analyse porosimetry curves and obtain compressibility parameters related to macropores that are suitable for lateritic soils.

2. Materials and methods

The soil used in this research is a residual weathered soil reddish in colour with characteristics of lateritic soils. XRD tests on these samples show a predominance of gibbsite and quartz minerals, and to a lesser extent, kaolinite and hematite (Guimarães, 2002). This material presents liquid limit, w_L, of 42%, plastic limit, w_P, of 24%, plasticity index, PI, of 18%, and specific gravity, Gs, of 2.748. It is classified as a low plasticity clay (CL) according to Unified Soil Classification System (ASTM, 2017). For this study, samples were collected at a depth of 1.7 to 2.3m and prepared under three different conditions: intact (I), compacted (C) and reconstituted (R) (**Figure 1a).**

Figure 1b shows the particle size distribution of tests performed with and without dispersant. Particle size distribution of sandy clay is observed in tests carried out with dispersant while silty sand distribution is observed in tests without dispersant. This difference is indicative of soils with aggregations formed by the cementation of smaller particles, which are stable in the presence of water but can be broken with dispersant (Camapum de Carvalho *et al.*, 2006; Ng, Akinniyi & Zhou, 2020; Otálvaro, Cordão-Neto & Caicedo, 2015).

Downloaded by [University of Strathclyde] on [22/10/21]. Copyright © ICE Publishing, all rights reserved.

Accepted manuscript doi:
10.1680/jgele.21.00063

The compressibility of the samples was assessed by means of oedometric tests following D2435 standard (ASTM, 2020). Specimens (I, C and R) of approximately 1 cm³ were moulded from freshly prepared (σ'_v = 0 kPa) samples and from samples that underwent vertical stresses of 50, 100, 200, 400 and 800 kPa. These specimens were subjected to freeze-drying and their pore size distributions were evaluated by means of Mercury Intrusion Porosimetry (MIP) tests using Autopore IV 9500 Micromeritics equipment.
It is important to note that the MIP technique has limitations (Romero & Simms, 2008), which make the void ratio obtained in this test different from the void ratio of the sample. **Table 1** presents the final void ratios intruded by mercury (e_{MIP}) and the void ratio of the samples (e_{sample}) for each stress level considered. This difference may have an impact on the fabric parameters as discussed later in this paper.
A fitting equation as proposed by Durner (1994) and Lopes, Cordão-Neto & Tarantino (2014), based on van Genuchten (1980)'s equation, was used to fit the MIP intrusion data.

$$e_{MIP} = e_{macro}\left[\frac{1}{1+\left(\alpha_{macro}.D\right)^{n_{macro}}}\right]^{1-\frac{1}{n_{macro}}} + e_{micro}\left[\frac{1}{1+\left(\alpha_{micro}.D\right)^{n_{micro}}}\right]^{1-\frac{1}{n_{micro}}} \quad (1)$$

where: D is the pore diameter intruded, μm, e_{macro} and e_{micro} are the void ratios of macro and micropores respectively, α_{macro} and α_{micro} are the fitting parameters related to the size of dominant macro and micropores respectively, μm^{-1}, and n_{macro} and n_{micro} (dimensionless) are the fitting parameters related to the slope of the macro and micropores intrusion curves, respectively.

The separation between macro and micropores was performed by best fitting of Eq. 1 which is highlighted in **Figure 3**. The R^2 of the fittings ranged from 0.98 to 1.00.

3. Results

3.1 Compressibility

Oedometric compression tests are presented in **Figure 2** while compressibility parameters (preconsolidation stress, σ'_{pc}, compression index, Cc, and recompression index, Cr) are presented in **Table 2**. It can be observed that the sample preparation conditions strongly affected the compressibility. The intact sample shows the highest compressibility due to its more porous structure. On the other hand, compacted and reconstituted samples present lower compressibility, as compaction or mixing at high water content during preparation stage caused structural alteration on those samples. In general, it is noticed that the initial structure has a relevant role in the compressibility of the samples.

3.2 Pore size distribution

Figure 3a, c, e show the cumulative intrusion curves of the samples (I, R and C) and **Figure 3b, d, f** present their respective pore size distributions. All samples show a bimodal behaviour for all loading stages investigated, with loading having the greatest impact on macropores. Without loading, the intact sample has larger macropores in respect to compacted and reconstituted samples, which is typical of collapsible soils (Camapum de Carvalho *et al.*, 2006). This shows that preparation conditions have strong impact on the pore size distribution and its evolution with loading, particularly decreasing the volume and dominant diameter of the macropores (**Table 1)**. The limiting diameter between macro and micropores is different from sample to sample and according to loading, as shown in **Figure 3**.

Downloaded by [University of Strathclyde] on [22/10/21]. Copyright © ICE Publishing, all rights reserved.

Accepted manuscript doi:
10.1680/jgele.21.00063

4. Evolution of fabric parameters with loading

The compression curves of the macro and micropores were determined based on macro and micro void ratios obtained through MIP tests for the different applied stresses. **Figure 4** shows the oedometric, macro and micropores compression curves, where the compression index of the virgin portion of the oedometric test (Cc - dimensionless), as well as the compression index of the macro (Cc_{macro} - dimensionless) and micropores (Cc_{micro} - dimensionless) are highlighted. These values are also presented in **Table 2**. The shape of the compression curve of the macropores is very similar to the compression curve of the samples, that is, the compressibility of the macropores predominates over the micropores, as observed by the Cc_{macro} values in **Table 2**.

The largest variations in macropores occur after the preconsolidation stress for intact and compacted samples. This observation leads to the conclusion that plastic deformations are mostly associated with deformations of the macropores. It is then reasonable to say that the process by which the largest pores close is irreversible. However, in the reconstituted samples, the trend of reduction of the macropores, as well as the compressibility curve of the sample are almost constant, with no occurrence of preconsolidation stress. Meanwhile, the void ratio of the micropores shows little variation due to loading, which may be related to the nature of the aggregations with smaller and cemented particles. Thus, it is possible to assume that the compressibility of the samples is largely related to the deformation of the macropores while the micropores remain mostly unaffected.

Delage (2010) found that the pore uniformity, given by the slope of the mercury intrusion curve (Cp index), has a good correlation with the compressibility (Cc) of some unimodal soils. The analyses performed by Delage (2010) were adapted in this work to bimodal soils. Thus, two coefficients were established: Cp_{macro} and Cp_{micro} for macro and micropores, respectively. **Figure 5** shows the evolution of the parameters for intact samples under 3 different stress levels. There is a change in the parameters, with a significant decrease in Cp_{macro}, indicating that the macropores are becoming well graded. The same behaviour in terms of macropores is seen in the other samples (see Cp_{macro} in **Table 1**). On the other hand, Cp_{micro} shows decreasing uniformity (**Figure 3** and **Table 1**). Thus, the behaviour of the macropores appears to be more significant than the modifications observed for the micropores.

Figure 6 shows the changes in parameter Cp_{macro} for each level of vertical stress, together with the compression curves of the sample and macropores. Since the dominant macropores change with loading, parameter Cp shows a different behaviour from that observed by Delage (2010) for St Marcel Clay. In this sense, it is necessary to establish a new index that can represent the change in the uniformity of each pore size for a given increase in stress, in which:

$$Cuc_{macro} = \frac{\Delta Cp_{macro}}{\Delta Log\sigma'_v} \qquad (2)$$

$$Cuc_{micro} = \frac{\Delta Cp_{micro}}{\Delta Log\sigma'_v} \qquad (3)$$

where: Cp_{macro} and Cp_{micro} (dimensionless) are the slope of the intrusion curve in the region of macro and micropores respectively, i.e., $Cp = \Delta e_{MIP} / \Delta LogD$; σ'_v is the effective stress, kPa; and Cuc_{macro} and Cuc_{micro} (dimensionless) are the macro and micropores index of uniformity

Downloaded by [University of Strathclyde] on [22/10/21]. Copyright © ICE Publishing, all rights reserved.

Accepted manuscript doi:
10.1680/jgele.21.00063

change, respectively. Cuc index is an indirect measure of how the compression coefficient varies with pore diameter, as follows:

$$Cuc_{macro} = \frac{\Delta Cp_{macro}}{\Delta Log\sigma'_v} \quad (4)$$

$$Cuc_{macro} = \frac{(Cp_{macro})_i - (Cp_{macro})_j}{\Delta Log\sigma'_v} \quad (5)$$

$$Cuc_{macro} = \frac{(\Delta e_{macro} / \Delta LogD)_i - (\Delta e_{macro} / \Delta LogD)_j}{\Delta Log\sigma'_v} \quad (6)$$

If $\Delta Log\ D$ intervals are the same, then:

$$Cuc_{macro} = \frac{(\Delta e_{macro} / \Delta Log\sigma'_v)_i - (\Delta e_{macro} / \Delta Log\sigma'_v)_j}{\Delta LogD} \quad (7)$$

$$Cuc_{macro} = \frac{(Cc_{macro})_i - (Cc_{macro})_j}{\Delta LogD} \quad (8)$$

$$Cuc_{macro} = \frac{\Delta Cc_{macro}}{\Delta LogD} \quad (9)$$

where: *i* and *j* represent same state (I, R or C) samples that underwent MIP tests at different loading stages.

Values of Cuc_{macro} and Cuc_{micro} are presented in **Table 2**. These were calculated between Cp at stresses of 400 and 800 kPa, as this is the stress range used to derive Cc. Higher values of Cuc_{macro} indicate that the pores of the macrostructure change easily and thus they can be related to compressible soils (higher Cc_{macro}). In contrast, smaller Cuc_{macro} values indicate less compressible soils (lower Cc_{macro}). Cuc_{micro}, on the other hand, presents negative values, indicating an increase in uniformity. It is important to note that the relationship between compressibility (Cc) and fabric parameters (Cc_{macro} and Cuc_{macro}) will be as good as the relationship between the void ratio of the sample (e) and the MIP void ratio (e_{MIP}). In this sense, it is not a surprise that the relationship between the fabric macro parameters and the sample compressibility of the compacted and reconstituted samples are better than that of the intact sample (**Table 1** and **Figure 7**). Excluding the intact sample, the correlation between Cc and Cuc_{macro} is satisfactory (**Figure 7**, $R^2 = 0.91$ for the y = x regression line). The introduction of macro and micro Cuc parameters do not make the use of Cc_{macro} and Cc_{micro} inappropriate. However, as previously discussed, Cuc has interesting physical meanings that could be further explored.

5. Conclusions

This paper evaluated the fabric modifications of a lateritic soil under different conditions of preparation (Intact, Reconstituted and Compacted). From the tests carried out, relationships were established between the compressibility parameters commonly used in geotechnics, such as: the compression index and preconsolidation stress, and fabric parameters of the soil. In this sense, new parameters have been proposed: (1) Cc_{macro} and Cc_{micro} that represent the compressibility of macro and micropores respectively, (2) Cp_{macro} and Cp_{micro} that represent the uniformity of macro and micropores respectively, (3) Cuc_{macro} and Cuc_{micro} that represent the change in the uniformity of macro and micropores, respectively.

The following points can be highlighted in respect to the soil under study:

(1) The compressibility of the sample is dominated by the compressibility of the macrostructure, that is, Cc_{macro} is very similar to Cc for compacted and reconstituted

Downloaded by [University of Strathclyde] on [22/10/21]. Copyright © ICE Publishing, all rights reserved.

Accepted manuscript doi:
10.1680/jgele.21.00063

samples. For the intact sample the difference between e_{MIP} and e results in the discrepancy observed between Cc and Cc_{macro}. The contribution of Cc_{micro} towards the compressibility of the sample is irrelevant.

(2) The uniformity of the pores changes during loading. However, the uniformity of the macropores (Cp_{macro}) is more affected by loading than the uniformity of the micropores (Cp_{micro}).

(3) Samples with higher macropores index of uniformity change (Cuc_{macro}) also present greater compressibility (Cc) and, consequently, higher compressibility of the macrostructure (Cc_{macro}).

Further studies with a wider range of soils may contribute to the verification of the correlations between the parameters discussed here.

Acknowledgements

The authors would like to thank Universidad de los Andes for providing access to their porosimeter.

List of notations

σ'_{pc} preconsolidation stress

σ'_{v} vertical effective stress

I intact sample

R reconstituted sample

C compacted sample

Cc sample compression index

Cc_{macro} macropores compression index

Cc_{micro} micropores compression index

Cp sample mercury intrusion curve slope angle

Cp_{macro} macropores mercury intrusion curve slope angle

Cp_{micro} micropores mercury intrusion curve slope angle

Cuc_{macro} macropore index of uniformity change

Cuc_{micro} micropore index of uniformity change

Cr recompression index

w_L liquid limit

w_P plastic limit

PI plastic index

Gs specific gravity

CL low plasticity clay according to Unified Soil Classification System

e_{sample} sample void ratio

e_{MIP} final MIP void ratio

D diameter of intruded pore

Downloaded by [University of Strathclyde] on [22/10/21]. Copyright © ICE Publishing, all rights reserved.

Accepted manuscript doi:
10.1680/jgele.21.00063

Dd_{macro} dominant macropore diameter

Dd_{micro} dominant micropore diameter

α_{macro} fitting parameter related to the size of dominant macropore

α_{micro} fitting parameter related to the size of dominant micropore

n_{macro} fitting parameter related to the slope of the macropore intrusion curve

n_{micro} fitting parameter related to the slope of the micropore intrusion curve

References

Alonso, E.E., Pinyol, N.M. & Gens, A. (2013) Compacted soil behaviour: initial state, structure and constitutive modelling. *Géotechnique*. [Online] 63 (6), 463–478. Available from: doi:10.1680/geot.11.P.134.

ASTM (2020) D2435 / D2435M-11. Standard Test Methods for One-Dimensional Consolidation Properties of Soils Using Incremental Loading. *ASTM International*. [Online] 1–11. Available from: doi:10.1520/D2435_D2435M-11R20.

ASTM (2017) *D2487-17e1, Standard Practice for Classifcation of Soils for Engineering Purposes (Unifed Soil Classifcation System).*

Burland, J.B. (1990) On the compressibility and shear strength of natural clays. *Géotechnique*. [Online] 40 (3), 329–378. Available from: doi:10.1680/geot.1990.40.3.329.

Camapum de Carvalho, J., Martines Sales, M., Moreira de Sousa, N. & da Silva Melo, M. (2006) *Erosive Processes in Central-West Brazil (in portuguese).* 1° ed. University of Brasilia - FINATEC.

Cordão Neto, M.P., Hernández, O., Lorenzo Reinaldo, R., Borges, C., et al. (2018) Study of the relationship between hydro-mechanical soil behavior and microstructure of a structured soil. *Earth Sciences Research Journal*. [Online] 22 (2), 91–101. Available from: doi:10.15446/esrj.v22n2.65640.

Delage, P. (2010) A microstructure approach to the sensitivity and compressibility of some Eastern Canada sensitive clays. *Géotechnique*. [Online] 60 (5), 353–368. Available from: doi:10.1680/geot.2010.60.5.353.

Delage, P., Audiguier, M., Cui, Y.-J. & Howat, M.D. (1996) Microstrucure of a compacted silt. *Can. Geotech. J.* 33, 150–158.

Delage, P., Marcial, D., Cui, Y.J. & Ruiz, X. (2006) Ageing effects in a compacted bentonite: A microstructure approach. *Geotechnique*. [Online] 56 (5), 291–304. Available from: doi:10.1680/geot.2006.56.5.291.

Durner, W. (1994) Hydraulic conductivity estimation for soils with heterogeneous pore structure. *Water Resources Research*. [Online] 30 (2), 211–223. Available from: doi:10.1029/93WR02676.

van Genuchten, M.T. (1980) A Closed-form Equation for Predicting the Hydraulic Conductivity of Unsaturated Soils. *Soil Science Society of America Journal*. [Online] 44 (5), 892–898. Available from: doi:10.2136/sssaj1980.03615995004400050002x.

Downloaded by [University of Strathclyde] on [22/10/21]. Copyright © ICE Publishing, all rights reserved.

Accepted manuscript doi:
10.1680/jgele.21.00063

Guimarães, R.C. (2002) *Analysis of the properties and behaviour of a laterite soil profile applied to the study of the performance of excavated piles (in portuguese)*. University of Brasilia.

Kochmanová, N. & Tanaka, H. (2011) Influence of the Soil Fabric on the Mechanical Properties of Unsaturated Clays. *Soils and Foundations*. [Online] 51 (2), 275–286. Available from: doi:10.3208/sandf.51.275.

Koliji, A., Vulliet, L. & Laloui, L. (2010) Structural characterization of unsaturated aggregated soil. *Canadian Geotechnical Journal*. [Online] 47 (3), 297–311. Available from: doi:10.1139/T09-089.

Kühn, V. de O., Lopes, B. de C.F.L., Caicedo, B. & Cordão-Neto, M.P. (2021) Micro-structural and volumetric behaviour of bimodal artificial soils with aggregates. *Engineering Geology*. [Online] 288 (April), 106139. Available from: doi:10.1016/j.enggeo.2021.106139.

Lambe, T.W. & Whitman, R. V. (1969) *Soil Mechanics*. [Online]. CRC Press. Available from: http://www.crcnetbase.com/doi/abs/10.1201/b15620-17.

Leroueil, S. & Vaughan, P.R. (1990) The general and congruent effects of structure in natural soils and weak rocks. *Géotechnique*. [Online] 40 (3), 467–488. Available from: doi:10.1680/geot.1990.40.3.467.

Lopes, B., Cordão-Neto, M.P. & Tarantino, A. (2014) An approach to detect microand macro-porosity from MIP data. In: *Unsaturated Soils: Research & Applications*. [Online]. CRC Press. pp. 685–689. Available from: doi:10.1201/b17034-96.

Miguel, M.G. & Bonder, B.H. (2012) Soil–Water Characteristic Curves Obtained for a Colluvial and Lateritic Soil Profile Considering the Macro and Micro Porosity. *Geotechnical and Geological Engineering*. [Online] 30 (6), 1405–1420. Available from: doi:10.1007/s10706-012-9545-y.

Mitchell, J.K. & Soga, K. (2005) *Fundamentals of Soil Behavior*. 3rd Editio. John Wiley and Sons.

Ng, C.W.W., Akinniyi, D.B. & Zhou, C. (2020) Influence of structure on the compression and shear behaviour of a saturated lateritic clay. *Acta Geotechnica*. [Online] 1. Available from: doi:10.1007/s11440-020-00981-1.

Ng, C.W.W., Mu, Q.Y. & Zhou, C. (2017) Effects of soil structure on the shear behaviour of an unsaturated loess at different suctions and temperatures. *Canadian Geotechnical Journal*. [Online] 54 (2), 270–279. Available from: doi:10.1139/cgj-2016-0272.

Ng, C.W.W., Sadeghi, H., Jafarzadeh, F., Sadeghi, M., et al. (2020) Effect of microstructure on shear strength and dilatancy of unsaturated loess at high suctions. *Canadian Geotechnical Journal*. [Online] 57 (2), 221–235. Available from: doi:10.1139/cgj-2018-0592.

Otálvaro, I.F., Cordão-Neto, M.P. & Caicedo, B. (2015) Compressibility and microstructure of compacted laterites. *Transportation Geotechnics*. [Online] 5 (October), 20–34. Available from: doi:10.1016/j.trgeo.2015.09.005.

Otálvaro, I.F., Neto, M.P.C., Delage, P. & Caicedo, B. (2016) Relationship between soil structure and water retention properties in a residual compacted soil. *Engineering*

Downloaded by [University of Strathclyde] on [22/10/21]. Copyright © ICE Publishing, all rights reserved.

Accepted manuscript doi:
10.1680/jgele.21.00063

Geology. [Online] 205 (August), 73–80. Available from: doi:10.1016/j.enggeo.2016.02.016.

Pedrotti, M. & Tarantino, A. (2014) Microstructural interpretation of compression behaviour of compacted kaolin clay. In: *Unsaturated Soils: Research & Applications*. [Online]. CRC Press. pp. 739–745. Available from: doi:10.1201/b17034-104.

Romero, E. (2013) A microstructural insight into compacted clayey soils and their hydraulic properties. *Engineering Geology*. [Online] 165, 3–19. Available from: doi:10.1016/j.enggeo.2013.05.024.

Santos, R.A. dos & Esquivel, E.R. (2018) Saturated anisotropic hydraulic conductivity of a compacted lateritic soil. *Journal of Rock Mechanics and Geotechnical Engineering*. [Online] 10 (5), 986–991. Available from: doi:10.1016/j.jrmge.2018.04.005.

Sivakumar, V. & Wheeler, S.J. (2000) Influence of compaction procedure on the mechanical behaviour of an unsaturated compacted clay. Part 1: Wetting and isotropic compression. *Géotechnique*. [Online] 50 (4), 359–368. Available from: doi:10.1680/geot.2000.50.4.359.

Wang, J.D., Li, P., Ma, Y., Vanapalli, S.K., et al. (2020) Change in pore-size distribution of collapsible loess due to loading and inundating. *Acta Geotechnica*. [Online] 15 (5), 1081–1094. Available from: doi:10.1007/s11440-019-00815-9.

Yu, C.Y., Chow, J.K. & Wang, Y.H. (2016) Pore-size changes and responses of kaolinite with different structures subject to consolidation and shearing. *Engineering Geology*. [Online] 202, 122–131. Available from: doi:10.1016/j.enggeo.2016.01.007.

Table 1. Sample data: e_{sample}, e_{MIP}, Dd_{macro}, Dd_{micro}, Cp_{macro}, Cp_{micro}

Sample	Consolidation		MIP				
	σ'_v (kPa)	e_{sample}	e_{MIP}	Dd_{macro}	Dd_{micro}	Cp_{macro}	Cp_{micro}
I	0	1.733	1.455	38.630	0.033	1.154	0.398
	50	1.636	1.255	17.083	0.027	0.600	0.552
	100	1.483	1.053	6.977	0.025	0.423	0.719
	200	1.286	1.060	6.771	0.026	0.478	0.668
	400	1.094	0.939	3.618	0.025	0.344	0.734
	800	0.887	0.820	1.972	0.023	0.240	0.777
C	0	1.149	1.065	24.933	0.031	0.834	0.490
	50	1.073	0.989	22.348	0.028	0.635	0.589
	100	1.049	1.011	15.465	0.030	0.520	0.528
	200	0.995	0.931	9.497	0.026	0.408	0.644
	400	0.896	0.941	8.513	0.028	0.394	0.594
	800	0.778	0.812	4.458	0.027	0.271	0.659
R	0	1.180	0.967	11.822	0.030	0.589	0.640
	50	0.885	0.869	7.630	0.027	0.305	0.726
	100	0.812	0.816	7.555	0.027	0.262	0.720
	200	0.728	0.744	3.957	0.028	0.242	0.680
	400	0.659	0.677	2.382	0.028	0.196	0.730
	800	0.591	0.661	1.648	0.026	0.131	0.763

Downloaded by [University of Strathclyde] on [22/10/21]. Copyright © ICE Publishing, all rights reserved.

Accepted manuscript doi:
10.1680/jgele.21.00063

Table 2. Compressibility and fabric parameters: σ'_{pc}, Cr, Cc, Cc_{macro}, Cc_{micro}, Cuc_{macro}, Cuc_{micro}

Sample	Compressibility parameters			Fabric Parameters			
	σ'_{pc} (kPa)	Cr	Cc	Cc_{macro}	Cc_{micro}	Cuc_{macro}	Cuc_{micro}
I	40	0.004	0.662	0.339	0.061	0.344	-0.145
C	90	0.003	0.392	0.363	0.066	0.410	-0.215
R	-	0.002	0.253	0.155	0.076	0.216	-0.109

Figure captions

Figure 1. (a) Compaction Curve and study points; (b) Particle size distribution.

Figure 2. Oedometric compression curves.

Figure 3. MIP tests of intact samples: (a) cumulative curves, (b) PSD; compacted samples: (c) cumulative curves, (d) PSD; reconstituted samples: (e) cumulative curves, (f) PSD.

Figure 4. Compression curves of whole sample, macroporosity and microporosity: (a) Intact; (b) Compacted; (c) Reconstituted.

Figure 5. Cp_{macro} and Cp_{micro} determination in cumulative mercury intrusion curve of intact samples.

Figure 6. Cuc_{macro}, Cp_{macro} and Cc: (a) Intact; (b) Compacted; (c) Reconstituted.

Figure 7. Relationship between Cuc_{macro}, Cc_{macro} and Cc.

Downloaded by [University of Strathclyde] on [22/10/21]. Copyright © ICE Publishing, all rights reserved.

Accepted manuscript doi:
10.1680/jgele.21.00063

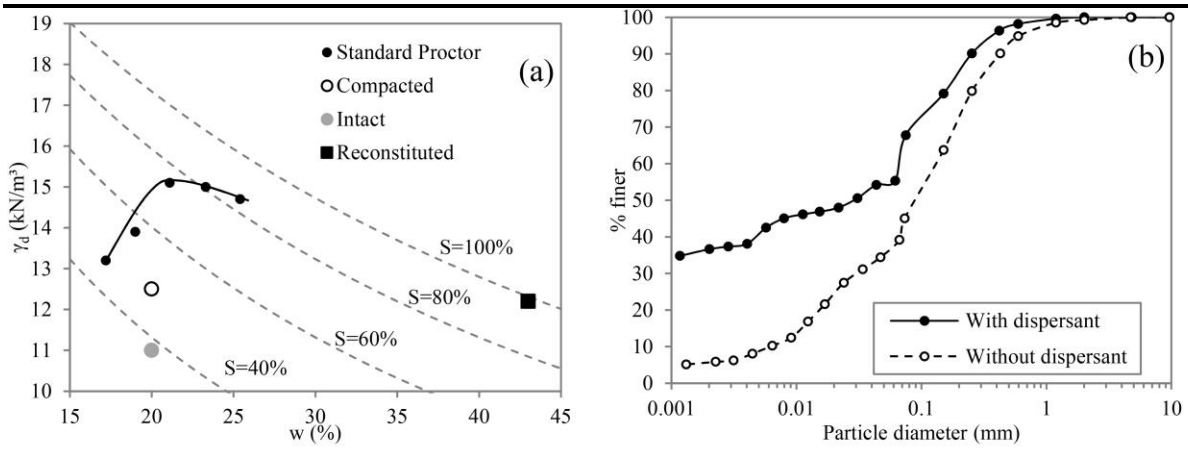

Figure 1

Downloaded by [University of Strathclyde] on [22/10/21]. Copyright © ICE Publishing, all rights reserved.

Accepted manuscript doi:
10.1680/jgele.21.00063

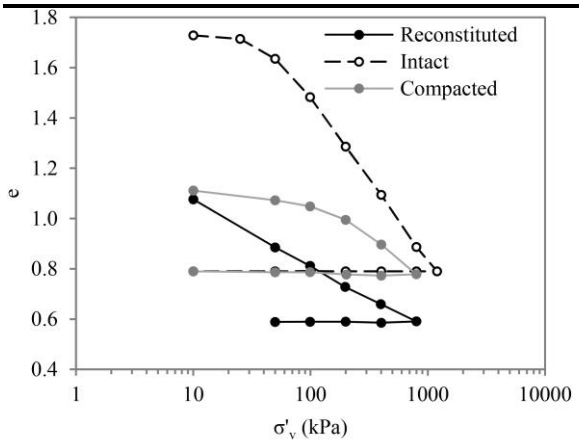

Figure 2

Downloaded by [University of Strathclyde] on [22/10/21]. Copyright © ICE Publishing, all rights reserved.

Accepted manuscript doi:
10.1680/jgele.21.00063

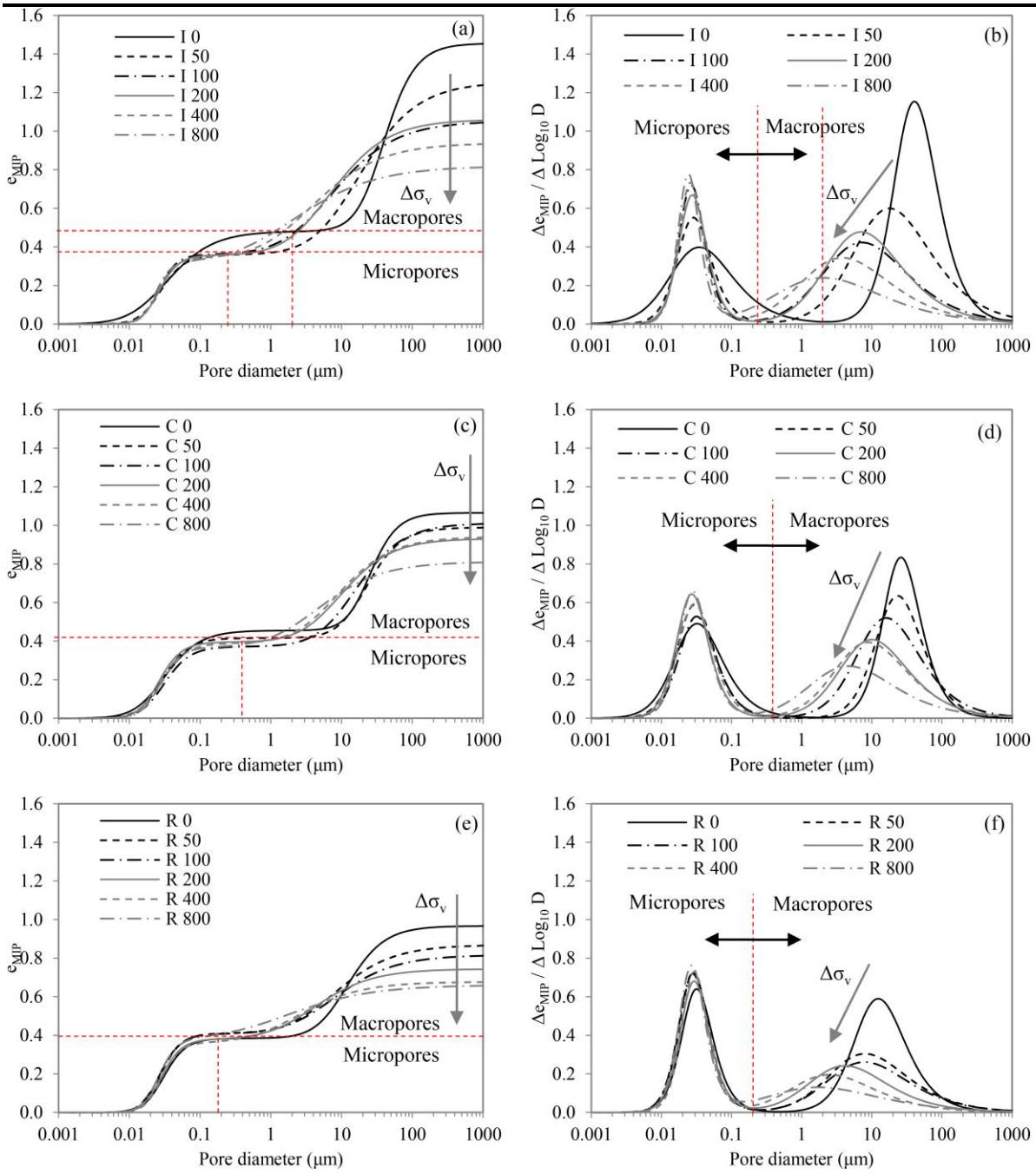

Figure 3

Downloaded by [University of Strathclyde] on [22/10/21]. Copyright © ICE Publishing, all rights reserved.

Accepted manuscript doi:
10.1680/jgele.21.00063

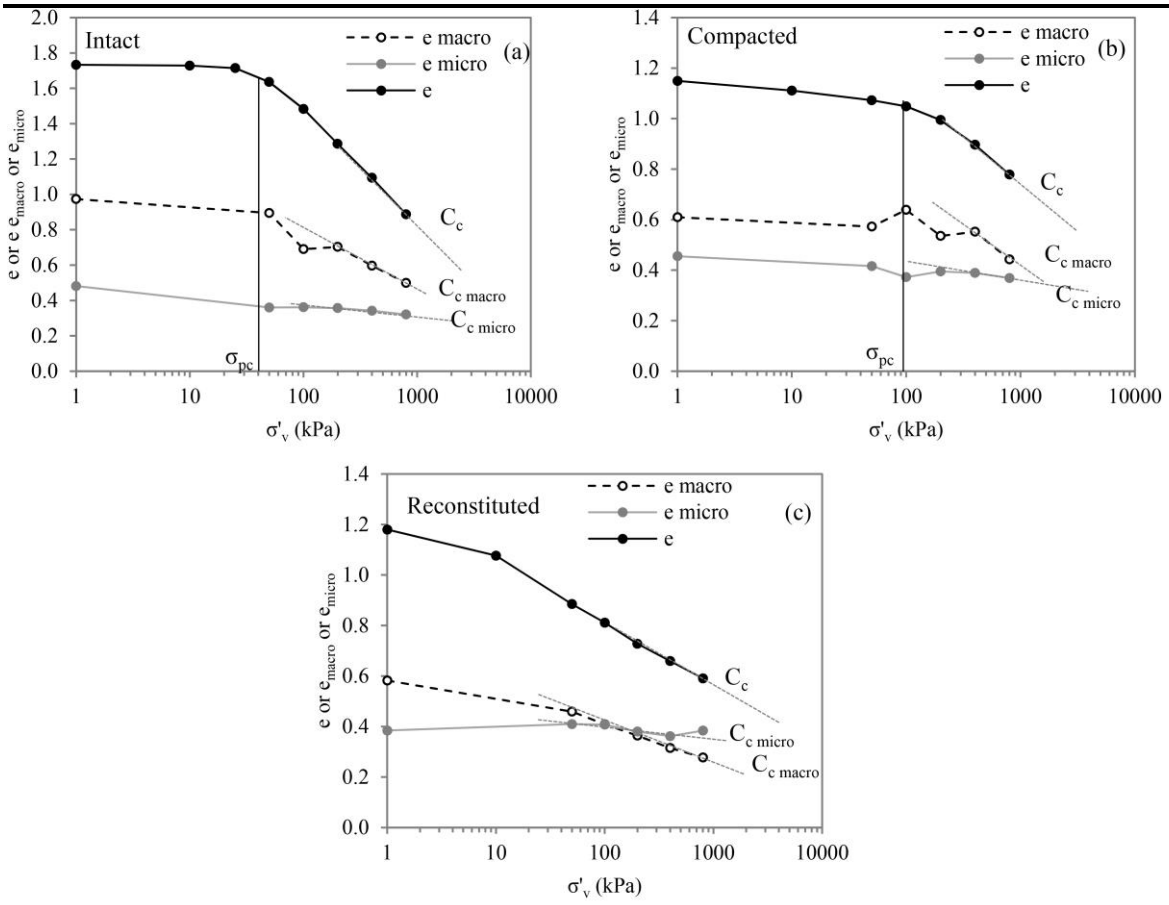

Figure 4

Downloaded by [University of Strathclyde] on [22/10/21]. Copyright © ICE Publishing, all rights reserved.

Accepted manuscript doi:
10.1680/jgele.21.00063

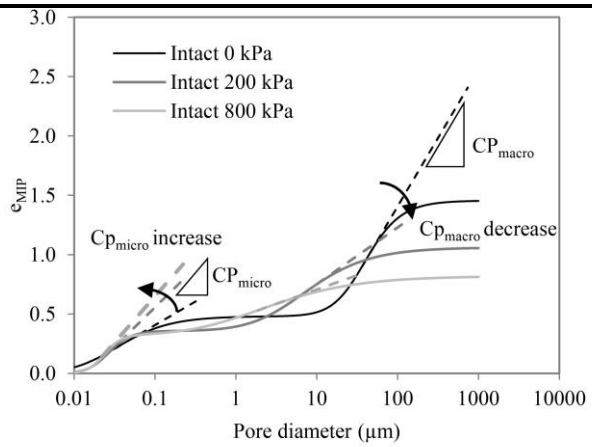

Figure 5

Downloaded by [University of Strathclyde] on [22/10/21]. Copyright © ICE Publishing, all rights reserved.

Accepted manuscript doi:
10.1680/jgele.21.00063

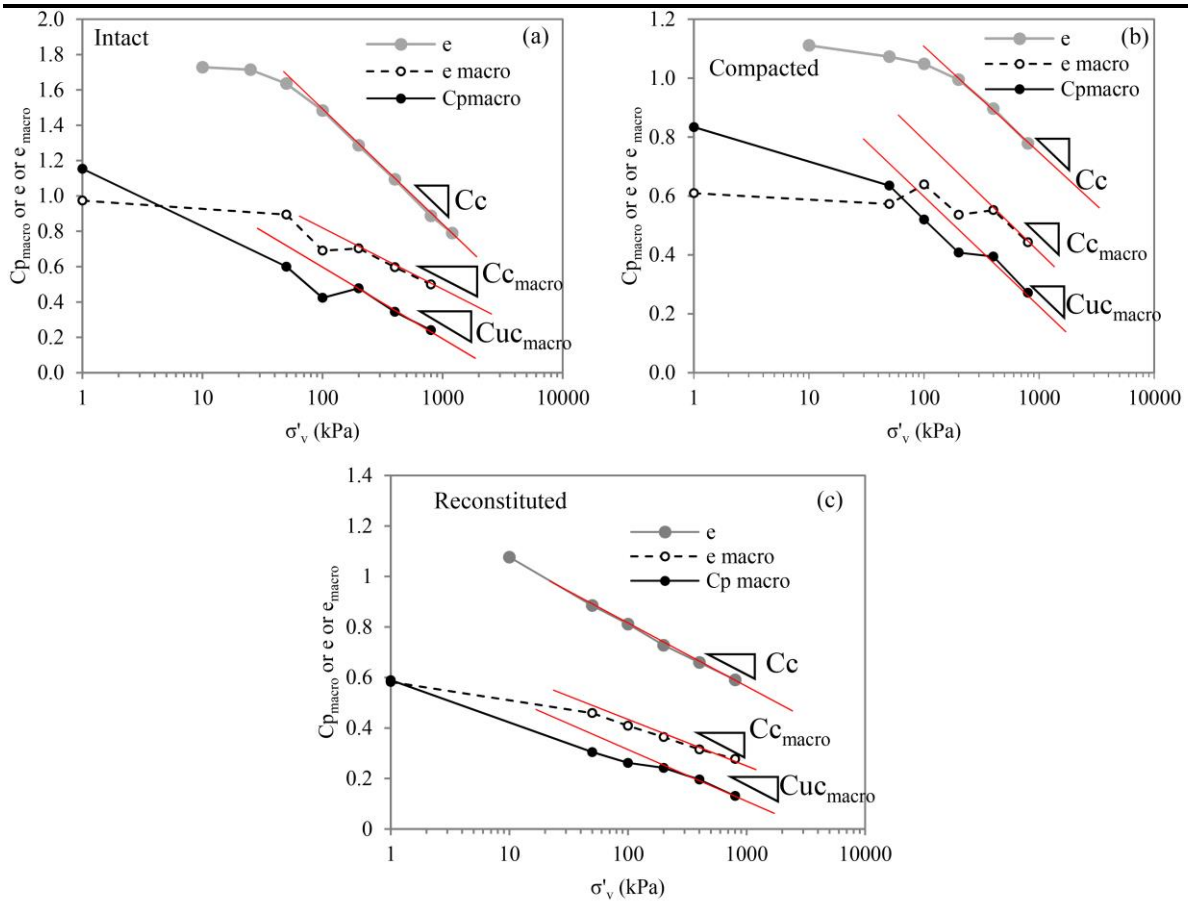

Figure 6

Downloaded by [University of Strathclyde] on [22/10/21]. Copyright © ICE Publishing, all rights reserved.

Accepted manuscript doi:
10.1680/jgele.21.00063

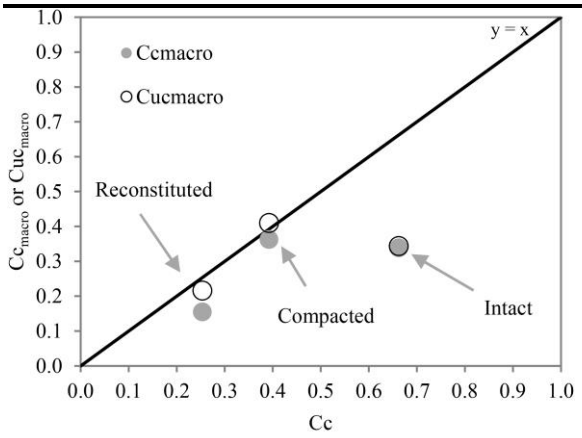

Figure 7.

Downloaded by [University of Strathclyde] on [22/10/21]. Copyright © ICE Publishing, all rights reserved.